Research Paper

Volume : 3 | Issue : 11 | November 2014 • ISSN No 2277 - 8179

Dielectric, thermal and rheological behaviour of graphene-PMMA nanocomposites

Chemistry

KEYWORDS : Graphene, PMMA, in-situ polymerization, dielectric studies

Manasi Singhi — Department of Chemistry, Ambedkar Institute of Advanced Communication Technologies and Research, Geeta Colony, New Delhi, India

*** M. Fahim** — Physics Department, Zakir Husain Delhi College, University of Delhi, New Delhi * Corresponding author

ABSTRACT

A series of graphene filled polymethylmethacrylate (PMMA) nanocomposites was prepared by in-situ polymerization in the laboratory. The concentration of graphene was changed in the step of 0.25 wt.% and nanocomposites were prepared in order to obtain a threshold concentration of graphene. These composites prepared by in-situ polymerization followed by compression moulding were characterized for their structural (using XRD, FT-IR), rheological, thermal (DSC, DT-TGA), dielectric behavior (∈', ∈") and ac conductivity. Frequency and temperature dependent behavior of dielectric constant was also studied. It was observed that at all temperatures and frequencies dielectric constant increased with temperature till it reached Tg and then decreased with further increase in temperature.It was observed that at room temperature composite with 0.75wt% of graphene showed a minimum value of dielectric constant at all frequencies.

1.0 Introduction

Small loadings of carbon-based nanofillers, such as carbon black (CB), expanded graphite (EG), graphite nanoplatelet (GNP), carbon nanotube (CNT) and graphene nanosheets (GNS) in non-conducting polymer matrices significantly improves the electrical conductivity of the latter **[1]**. CNTs are most effective as conductive fillers, however, their higher production cost is a constraint. Compared to CNTs, the two dimensional GNSs are not as effective in forming conductive networks due to the aggregation of GNSs in the polymer matrix but they are economically viable. Thus, in order to make optimum utilization of the advantages of GNSs as conductive fillers and derive high performances from resultant composites serious efforts have been made in the past **[1-3]**. A small loading of GNS not only ensures achievement of higher electrical conductivity but also helps in retaining the properties of the base polymer matrix **[4].** It has been reported that the percolation threshold of PMMA/graphite nanosheets conducting films, at room temperature, was as low as 0.31 vol% which was much lower than that (3.19 vol%) of the composites filled with conventional graphite filler particles. Their results also showed that the high aspect-ratio (width to thickness) structure of graphite nanosheets played an important role in forming conducting network in PMMA matrix **[5]**. Similarly, for PMMA/graphite nanoplatelet ensembles, the electrical conductivity of the ensemble was found to exhibit an insulator–conductor transition at a very low percolation threshold for GNPs **[6]**. The percolation threshold of PMMA/GNP at room temperature was only about 1 wt% filler content which is much lower than that of the ensembles filled with conventional graphite particles. GNP/PMMA nanocomposites show vastly improved conductivity as compared to ARG/PMMA and EG/PMMA nanocomposites **[7]**. In the case of a graphene nanosheet filled ultrahigh molecular weight polyethylene (UHMWPE) composite with a segregated structure fabricated by exfoliating graphene oxide nanosheet (GONS) and then water/ethanol mixture solvent-assisted dispersion under ultrasonication, a percolation threshold as low as 0.070 vol.% has been achieved because of the formation of a two dimensional conductive network **[8]**. Thus, from the literature survey, it was observed that *in-situ* polymerization is the best method to achieve optimum electrical conductivity and other properties in graphene filled PMMA nanocomposite presumably because graphene can easily exfoliate in MMA monomer by the help of ultra-sonication rather than in the polymer. Hence in this paper, we decided to synthesize the PMMA/Graphene nanocomposites, by *in-situ* polymerization of MMA monomer with the help of ultra-sonication,and characterize them for their structural, morphological, thermal, dielectric and electrical conductivity properties. The main objective of this research work is to obtain a very low percolation threshold concentration of graphene.

2.0 Materials and methods

Methyl methacrylate (MMA) (Density = 0.936g/cc and Purity = 99%) was obtained from Sigma Aldrich, Germany.Benzoyl peroxide (BPO) (Melting pt. = 54°C) was al,(Purity = 99.5%, Layer Flake = 4-6 (50-80%), Surface Area ≥ 250m2/g, Thickness =2-4nm, Lateral Size = 1-10μm, pH = 6-7, Ash ≤ 0.5%, Morphology = Flaky) was obtained from Nanoshel LLC. Firstly, *in-situ* polymerization of MMA monomer was carried out in test tubes with the help of ultra-sonication under suitable conditions. Exact amount of graphene was taken in dry test tubes and then it was sonicated for 5 minutes in dry condition. 10g of MMA monomer and 0.1g of BPO initiator were added to the test tubes. Nitrogen was purged for 1 minute in every test tube to create an inert atmosphere. Test tubes were plugged tightly with cotton and sonicated for 10 minutes at room temperature. Now, these systems were slowly heated to 60°C and sonicated for total 2 hours until the monomer system became viscous and graphene got entrapped into the polymer chains. After 2 hours, sonication was stopped and systems were heated for another 2 hours to complete the polymerization under nitrogen atmosphere. After 4 hours polymeric lumps were formed inside the test tube. Test tubes were then broken to take out the polymeric lumps. These polymer lumps were crushed at 20,000 lb pressure in compression moulding machine without heating. Thus, micro cracks developed inside the lumps and then they were granulated. Granules were dried at 60°C under vacuum for 24 hours to remove low molecular weight components. After that, granules were compression moulded to make samples at 165°C and at 15,000 lb pressure. Granules were preheated for 15 minutes and compression moulded for another 15 minutes with a breathing time of 30 seconds. Then, samples were slowly cooled to 65°C by circulating water inside the platen and then they were ejected from the mould. A total of 10 different samples were prepared by varying the weight percentage of graphene. The sample designation and composition is listed in **Table 1**.

2.1Raw Material Characterization:

Structural and thermal characterization of raw materials (PMMA and graphene) was done using GPC, DSC, TGA, DTGA, FTIR and XRD.

2.1.1. GPC Analysis of PMMA

Waters 1525, Binary HPLC Pump Instrument having THF as mobile phase, with Viscotek VE 3580 RI Detector was used to determine the molecular weight of pure PMMA **(Table2)** using poly-

styrene as calibration standard with 1 ml/min flow rate when column and detector temperature was at 35°C.

2.1.2 Thermal characterization of PMMA

Glass transition temperatures (Tg) of pure PMMA sample (PG000) and nanocomposites were examined by differential scanning calorimetry (DSC) using TA Instruments, DSC Q 200 machine, at heating rate 10°C/min and cooling rate 5°C/min. Thermal analysis of pure PMMA sample (PG000) was evaluated by recording thermo gravimetric traces using Perkin Elmer Thermogravimetric Analyser, Pyris 6 TGA machine at a temperature range of 50°C to 750°C and heating rate 20°C/min.

2.1.3. FT-IR Analysis

The FT-IR spectra of graphene nanopowder and pure PMMA (PG000) were recorded by using Thermo Scientific, Nicolet 6700 FT-IR machine. **Figure 1a** shows the FT-IR of graphene nanopowder and **Fig. 1b** shows the FT-IR of pure PMMA (PG000).The characteristic absorption peaks observed in graphene nanopowder were 3426.41, 2923.12, 1587.80, 1414.63, 1116.68 and 1036.52 cm-1and that observed in pure PMMA (PG000) were 2996.97, 2948.67, 1443.74, 1241.33 and 1149.30 cm-1. The groups responsible for these peaks were listed in **(Table 3) [9,10]**. FT-IR spectrographs of various samples were obtained on the same instrument and comparative values of the various functional groups and wavenumbers are given in **Table 3**. It is observed thatH-bonding in OH functionalized graphene structure is destroyed in nanocomposites. The peak of C=O stretching of PMMA is not shifted to lower value when Graphene is added into the medium which indicates the absence of H-bonding in resulting nanocomposites.

2.1.4 XRD Analysis

WAXRD tests were performed by using Philips XPERT-PRO instrument with Cu anode and K-alpha is 1.54 Å. The generator has a 40 mA current and 45 kV voltages. The compression molded samples of each composition was used for WAXRD experiments. The two theta (2θ) range was 2° to 40°. X-ray diffractograms of pure PMMA and graphene powder are shown in **Fig. 2 (a-c)**. It is observed from these figures that no definite peak exists showing the amorphous halo of polymer. It shows that the structure of PMMA is completely amorphous. In the case of graphene, a definite peak is observed at 2θ = 26.6905° at a d-spacing of 3.33725 Å. Due to 50-80% of layer flake structures (4-6 layers) peak intensity is very high.

2.1.5 Dielectric Study

AC frequency dependent values of parallel capacitance (Cp) and loss tangent or dissipation factor (tanδ or D) of the nanocomposite samples were measured by using Agilent 4263B precision LCR meter. The actual thickness of samples was measured using a micrometre before electroding by application of conductive silver paste using a paint brush. Electroded samples were placed in a sample cell between two electrodes and voltage was applied. The parallel capacitance (Cp) was measured on the LCR meter. Dielectric constant (ε′) was calculated using the formula:

$$\varepsilon' = C/C0$$

Where, Co (=ϵ0A/d) is the capacitance with vacuum between parallel plates, and ϵ0 is the permittivity of free space, A is the area of electrodes, and d is the thickness of the sample. Dissipation factor (D or tanδ) was directly measured on the LCR meter.

To calculate *ac* conductivity, parallel capacitance (Cp) and dissipation factor (D or tanδ) from 100 Hz up to 100 kHz was measured. σac(ω) was calculated by using the following expression:

$$\sigma ac(\omega) = 2\pi f \epsilon 0 \varepsilon'' = 2T\pi f \epsilon 0 \varepsilon' \tan\delta$$

Where, tanδ is the dissipation factor, ω=2πf is the angular frequency, ϵ0 is the permittivity of free space (=8.865×10-12 F/m), ε′ is the dielectric constant (ε″ /ε′ = tanδ), and ε″ is the dielectric loss.

1.0.6 Rheological Studies

Parallel plate rheological tests were performed using Bohlin C-VOR instrument. Samples were used in the form of compression moulded specimen of circular disc of 25 mm in diameter and 1 mm in thickness. The strain amplitude sweep and frequency sweep experiments of the nanocomposite samples were carried out parallel plate rheometer to study the strain and frequency dependence of Storage modulus (G′), Loss modulus (G″), tanδ and complex viscosity (η*).

3.0 Results and discussion

The results obtained from the DSC analysis are summarised in **Table 4**. From the DSC traces it was observed that the nanocomposite samples are totally amorphous and there is no crystallisation in the samples. In the temperature region between room temperature to 200°C only a prominent base line shift in the DSC plot is observed which corresponds to the glass transition temperature (Tg) of the samples. No other endotherms or exotherms observed in the DSC traces. In **Table 4** the values of the glass transition temperatures (Tg) of different samples show the variation of Tg with increase in Graphene wt. percentage. It is observed that Tg of the PMMA/Graphene nanocomposites decreases with increase in the wt. %age of Graphene. This phenomena can be described by Domain Relaxation Theory proposed recently by Lu and Nutt. According to this theory molecular structure can be divided into three regions: Domain I: a slowly relaxing domain which is confined to the Graphene layers where the PMMA molecules are tethered to Graphene layers. Domain II: a region of faster motion where the material is isolated from the bulk and from the tethered state, and thus relaxes faster (due to a lack of such interactions) and has been observed particularly in thermoplastic nanocomposites, such as by NMR. The final region (Domain III) is the bulk material, which has the same glass transition as if there were no added layers of Graphene. The ability to manipulate the size of these relative areas will vary the effect on Tg. Clearly greater exfoliation will result in more numbers of tethered molecules in Region II. At very low percentages of Graphene, layers are totally exfoliated and a large number of polymer molecules are tethered to the surface of Graphene and thus the volume available for relaxation of the bulk material increases and consequently Tg decreases. But as the nanofiller percentage increases, after a certain percentage of nanofiller restriction to mobility of the polymer chains dominates over Domain relaxation mechanism and so Tg starts to increase after 1 wt.% of Graphene **[11]**.

TGA & DTA Analysis

Table 4 also shows the analysis of TGA results. It was observed that the onset degradation temperature and thermal stability of PMMA/Graphene nanocomposites increases due to incorporation of Graphene. As the graphene percentage increases, onset of degradation temperature increases and thus the thermal stability of the nanocomposites also increases. It is also observed that end of degradation temperature shows a decreasing pattern for all the nanocomposites with increase in Graphene percentage though it rises at first due to incorporation of Graphene. The result obtained from DTA analysis shows that during degradation of PMMA/Graphene nanocomposites an endotherm occurs where the rate of degradation is maximum. Onset of this endotherm occurs at around 335-340°C and the peak of the endotherm occurs at around 370-375°C and also the peak shifted slowly towards the higher side with increase in the percentage of Graphene. The presence of endotherm during degradation might be due to the inert nitrogen environment. As there is no supply of oxygen, polymer samples cannot oxidise into CO2 and H2O. If

the sample will able to oxidise, then an exotherm should result. But in nitrogen atmosphere only unzipping of polymer PMMA is the major degradation mechanism. As the free energy of polymer is lower than that of the monomers, an additional heat to be supplied to the system during degradation which results in the endotherm in the DTA traces [12].

FT-IR Analysis

The IR absorption peaks of the PMMA/Graphene nanocomposites are listed in Table 3. FT-IR results show that there is a broad peak at 3426.41 cm-1 in Graphene which corresponds to the hydroxyl groups which are hydrogen bonded. In Graphene, there exists a planar form of large numbers of fused benzene ring and there should not be any hydrogen present in the structure. But when Graphenes are functionalised by hydroxyl groups the some of their carbon atoms becomes sp3 hybridised and thus hydrogen comes into the structure which are responsible for hydrogen bonding in Graphene. It is observed that, when Graphene is incorporated into the PMMA matrix then the O-H stretching peak of Graphene completely vanishes. This may be due to the exfoliation of Graphene in the polymer matrix during polymerization. Also, the peak of C=O stretching of PMMA is not shifted to lower value when Graphene is added into the medium. It indicates the absence of hydrogen bonding in the resulting nanocomposites. This peak remains almost unchanged with increase in Graphene percentage. Other peaks of PMMA (PG000) such as O-H stretching, C-H stretching, C-CH3 stretching, C-H bending and C-H stretching of ester also remains unchanged with the increase in Graphene concentration in the system which is expected.

WAXRD Analysis of nanocomposites

From WAXRD analysis it is observed that Graphene dispersion becomes more and more difficult with increasing Graphene loading as seen from the intensity of the WAXRD peaks. As Graphene loading increases, the intensity of the peak also increases slowly. The WAXRD plots of different samples are shown in **Fig. 2c.** The absence of any other peaks in the plots indicates that the samples are totally amorphous in nature. The very large decrease in the peak intensity of Graphene in the polymer nanocomposites indicates that only a very few layers of intercalated structure exist in the system.From the peak position values and d-spacing values, it can be seen that, peak position decreases with Graphene percentage upto a certain extent i.e., up to 1 wt% of Graphene and then it remains almost constant. Initially in Graphene it was at 26.6905° but whet it is incorporated into PMMA matrix then polymer molecules enter into the interlayer space of graphene and pushes the layers to separate them. And consequently d-spacing also increases upto 1wt% and then get almost constant. Shifting of peak positions to lower angles indicates intercalation of Graphene layers by polymer molecules and the characteristic amorphous halo in all compositions indicates the absence of ant crystallinity in the samples.

Dielectric Analysis

Frequency dependent dielectric behaviour of nanocomposites at room temperature is shown in **Fig. 3 (a-d)**.Figure 3 (a, b) shows the variation of dielectric constant (ε′) and dielectric loss (ε″) respectively with frequencies at room temperature (22°C).It can be seen that with increasing frequency dielectric constant (ε′), dielectric loss (ε″) decreases. This is because of the available relaxation time of the polymer. At low frequencies polymer molecules get sufficient time to orient themselves according to the applied field. But as the frequency increases molecules are not getting sufficient time to orient themselves according to the direction of the electrical field. Therefore, the overall polarization effect decreases and consequently the value of dielectric constant also decreases as it is directly proportional to the amount of polarization. At high frequencies as the polarization decreases the dielectric loss and dissipation factor, also decreases as sufficient time is not provided to the polymer chain to generate phase angle. Thus, at high frequencies the contribution of orientational or dipole polarization vanishes and the effect is only for electronic polarization which is instantaneous.

In **Fig. 3d**, room temperature (22°C) dielectric constants at different frequencies are plotted as a function of increasing Graphene weight percentage. It is expected that at lower frequencies the values of dielectric constant will be higher due to contribution of both electronic polarization and orientational or dipole polarization. With increase in frequencies orientational polarization is restricted but electronic polarization are not. Here it is observed that with increasing graphene percentage dielectric constant decreases and then reaches to a minimum and then start to increase but after 1.5 wt. % it falls slightly. This is because at a constant frequency when Graphene percentage increases then more and more restrictions are applied to the polymer molecule to polarization and consequently the contribution of orientational polarization decreases monotonically. But at very low percentage of graphene the enhancement in electronic polarization is suppressed by the decrease in dipole polarization and thus the overall polarization decreases resulting the decrease in dielectric constant value. But after a certain percentage the contribution of increase in electronic polarization and decrease in dipole polarization counter balance each other and after that the increase in electronic polarization becomes more significant. As a result of this phenomenon, dielectric constant reaches a minimum and the starts it increase. But after 1.5% Graphene loading it is observed that dielectric constant starts decrease slowly and this can be due to stabilization of electronic polarization after a certain concentration. So again the decrease in orientational polarization determines the nature of the curve **[13-16].**

Frequency dependence of ac-conductivity of composites at room temperature is shown in **Fig. 3c**. σac(ω) is the ac conductivity, which is frequency-dependent conductivity and it follows a universal power law, which is applicable for polymeric and semiconductor materials. Theσac(ω) obeys the universal power law in the form of:

$$\sigma ac(\omega) = A\omega^{s}$$

where, A is the dose-dependent coefficient, ω=2πf is the angular frequency and frequency exponent, s ($0 \le s \le 1$). The value of s can be determined from the linear slope of log σac(ω) versus log ω. Here with increasing frequency, ac conductivity of all composition increases according to the universal power law.

Temperature dependent capacitance (Cp) of PG100 nanocomposites is shown in **Fig. 4** at different frequencies. At all temperatures and frequencies it was observed that capacitance [and hence dielectric constant (ε′= C/C0)] increased with temperature till it reached Tg and then decreased with further increase in temperature. All composites showed similar pattern of dielectric behaviour.

Rheological Study

Figure 5a shows the plots of elastic modulus dependence of strain for PMMA (PG000) and PG250 at 180°C at a frequency of 1 Hz. It is indicated that the regions of linear viscoelastic behavior for PMMA (PG000) is wider than PG250 and behavior of the latter is sensitive due to the presence of Graphene. The linear viscoelastic regions for PMMA extend to a strain of 0.1 and that for PG250 is about 0.01 under the testing conditions. After those certain strains the curves starts to fall. Therefore, frequencysweep, to study the linear viscoelastic properties of PMMA/Graphene nanocomposites were conducted at a fixed strain of 0.005 at 180°C. It is also seen that elastic modulus exhibits a linear region at low strain amplitudes for both the samples; however, a noticeable nonlinear region at higher strain amplitudes

can be observed which is called Payne effect. This behaviour could be attributed to the formation of more strain-sensitive rigid network-like structures which rupture at higher strain amplitudes, leading to a narrower region of linear viscoelasticity. And in higher Graphene percentage network like structures are more which breaks at a lower strain than compared to the pure PMMA (PG000).Frequency sweep was done in the range of 0.01-100.0 (Hz) to study the rheological behaviour of nanocomposites in the linear viscoelastic region. The strain was kept at 0.005 at a temperature of 180°C.**Figure 5b and 5c**show the variation of storage modulus (G′) and loss modulus (G″) against frequency respectively. Comparison of the linear viscoelastic response of the materials shows the significant effect of the Graphene loading with frequency. As the graphene percentage increases, storage modulus and loss modulus of nanocomposites compared with pure PMMA shows a monotonic increase. The reason for the increase of storage modulus and loss modulus might arise from the confinement of polymer chains within the graphene layers. Due to incorporation of nano filler, increase of storage modulus (G′) is expected due to the additivity principle of modulus and it increases by a considerable amount with graphene percentage as low as 0.25 wt.%. In low percentage of filler the plot of PG025 follows the same nature as that of pure PMMA (PG000). But as the filler percentage increases the nature of the curve changes and they increases slowly throughout the entire frequency range. In case of loss modulus (G″), as nano filler percentage increases, the viscous part increases and consequently the loss modulus also increases. From the curves it is noticeable that loss modulus increases at higher frequencies.In **Fig. 5d**, it is observed that complex viscosity of nanocomposites decreases with increase in frequency. As with increase in graphene content the viscous part increases in the nanocomposites, viscosity of the nanocomposites are higher than that of pure PMMA (PG000) and it remains higher in the complete frequency range though the curves follow same decreasing nature with frequency **[17].**

4.0 Conclusions

Graphene filled PMMA nanocomposites were prepared using *in-situ* polymerization to obtain an optimum concentration of graphene to achieve desired properties in nanocomposites for specific application. It was observed that nanocomposites showed better properties due to homogeneous dispersion, intercalation and exfoliation of the graphene layers in the PMMA matrix. It was observed that the thermal stability of the nanocomposites improved due to graphene incorporation and exfoliation of graphene in resulting nanocomposites. At room temperature and at all frequencies dielectric constant (ε′) decreased with increasing concentration of graphene and reached a minimum at a filler concentration of 0.75 wt%. Rheological studies showed that the storage modulus (G′) improved with incorporation of graphene as nanofiller. Similarly, loss modulus (G″) and complex viscosity (η*) also increased with increasing graphene weight percentage.

Table 1: Sample designation and composition

Sample Name	PMMA (wt.%)	BPO (wt.%)	Graphene (wt.%)
PG000	100	1.00	0.00
PG025	100	1.00	0.25
PG050	100	1.00	0.50
PG075	100	1.00	0.75
PG100	100	1.00	1.00
PG125	100	1.00	1.25
PG150	100	1.00	1.50
PG175	100	1.00	1.75
PG200	100	1.00	2.00
PG250	100	1.00	2.50

Table 2: Molecular weight of pure PMMA determined using GPC

Sample	Property	Value
	M_n (g mol^{-1})	2,68,021
PG000	M_w(g mol^{-1})	8,33,736
	PDI (M_w/M_n)	3.111

Table 3: Comparative values of the various functional groups and corresponding wavenumbe obtained through FT-IR spectra for different samples

Sample Name	O-H Stretch	C-H Stretching	C=O Stretch	C-CH_3 Stretch	C-H Bending	C-H Bend (ester)
Graphene	3426 (br)	2923.12	1587.80			
PG000	3438.80	2996.97 2948.67	1729.61	1443.74	1241.33	1149.30
PG025	3438.62	2996.48 2948.11	1730.76	1444.36	1242.52	1150.44
PG050	3438.63	2998.30 2949.07	1734.73	1443.19	1242.36	1150.40
PG075	3438.73	2998.24 2949.14	1733.28	1443.72	1242.33	1150.28
PG100	3438.79	2997.77 2949.31	1730.65	1444.54	1242.43	1151.14
PG150	3439.31	2997.94 2949.32	1730.85	1444.67	1242.32	1151.05
PG175	3438.29	2995.98 2950.67	1731.63	1449.00	1242.01	1149.61
PG200	3439.01	2997.80 2949.23	1730.90	1444.52	1242.67	1151.23
PG250	3439.04	2997.48 2949.14	1730.58	1444.56	1242.76	1151.07

Table 4 TGA and DTA results of the PMMA/Graphene nanocomposites

Sample Name	DSC Data	TGA Data		DTA Data	
	Glass transition temperature (Tg) (°C)	Onset of Degradation T_{Onset} (°C)	End of Degradation T_{End} (°C)	Onset of Endotherm (°C)	Peak of Endotherm (°C)
PG000	108.24	170.81	423.91	336.49	376.20
PG025	105.97	170.12	436.23	346.06	370.59
PG050	103.96	171.61	430.03	341.79	373.72
PG075	103.30	174.32	430.49	338.74	374.04
PG100	100.29	174.49	442.84	339.17	374.38
PG150	102.56	177.06	419.83		
PG200	102.86	180.12	414.93		
PG250	102.44	181.66	421.60		

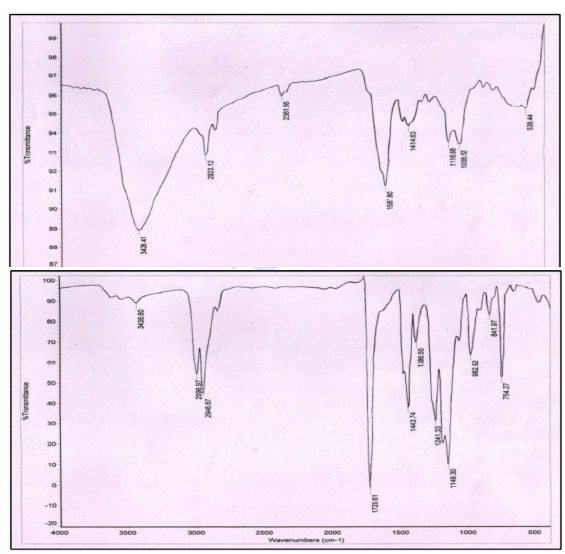

Figure 1 FT-IR of (a) Graphene Nanopowder and (b) pure PMMA (PG000)

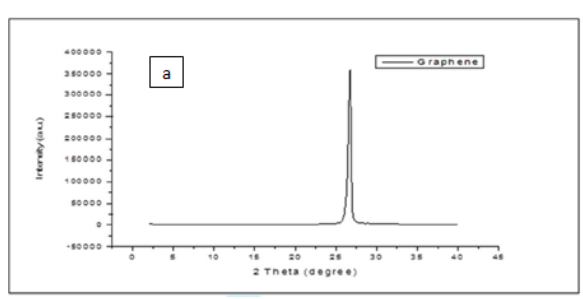

Volume : 3 | Issue : 11 | November 2014 • ISSN No 2277 - 8179

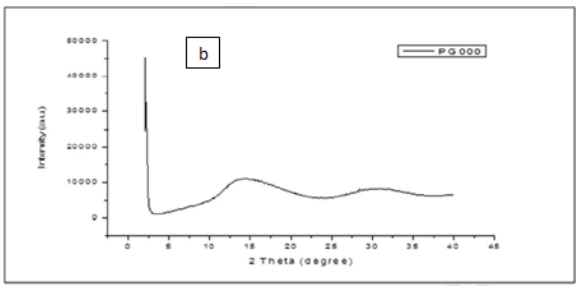

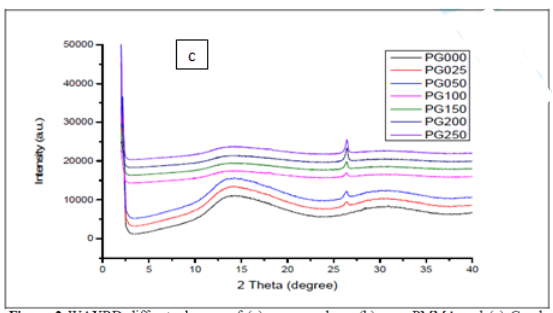

Figure 2 WAXRD diffractogram,s of (a) pure graphene (b) pure PMMA and (c) Graphene-PMMA nanocomposites

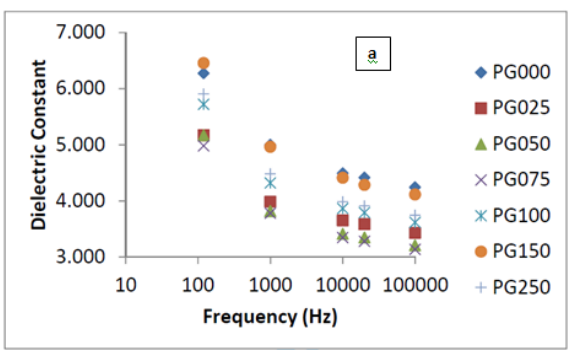

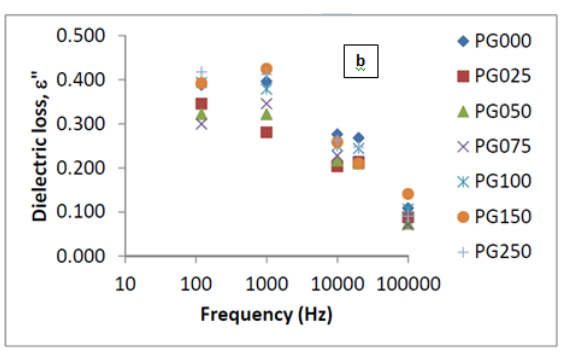

Figure 3 Frequency dependent dielectric behaviour of graphene-PMMA nanocomposites at room temperature (a) dielectric constant (b) dielectric loss

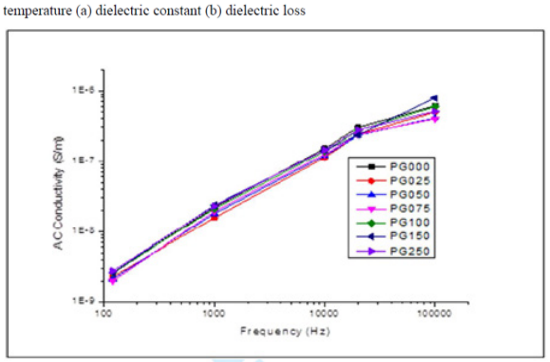

Fig. 3c : ac conductivity (σ_{ac}) of graphene - PMMA nanocomposites at different frequencies at room temperature

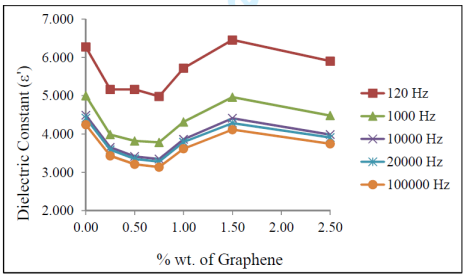

Fig. 3d: Variation of dielectric constant of nanocomposites as a function of graphene weight percentage at different frequencies

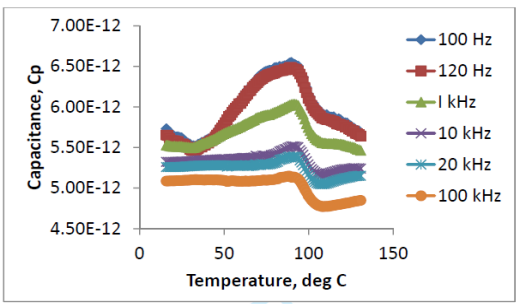

Fig. 4 : Temperature and frequency dependent Capacitance of PG100 nanocomposites

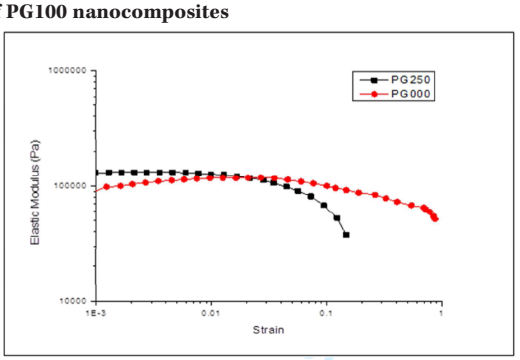

Fig. 5a : Elastic modules versus strain of PMMA and PG250 nanocomposite

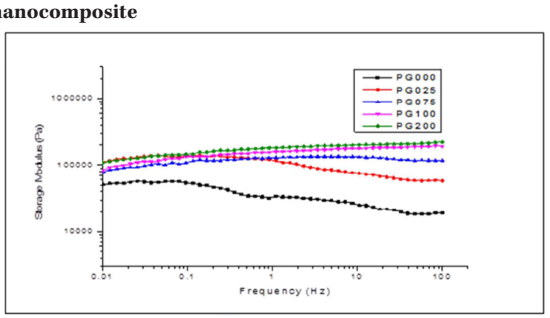

Fig. 5b : Storage modulus (G') versus frequency curve of different nanocomposites obtained at a strain of 0.005 at 180 deg C

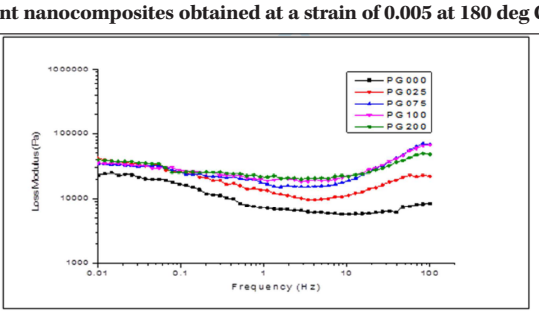

Fig. 5c: Storage modulus (G') versus frequency curve of different nanocomposites obtained at a strain of 0.005 at 180 deg C

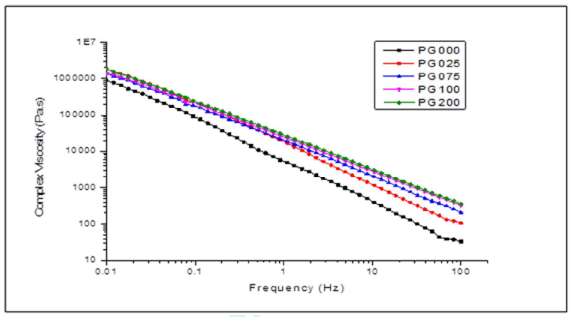

Fig 5d : Complex viscosity versus frequency curves of different nanocomposites at a strain of 0.005 at 180 deg C.

REFERENCE

Tapas Kuilla, SambhuBhadra, Dahu Yao, Nam Hoon Kim, Saswata Bose, JoongHee Lee; Recent advances in graphene based polymer composites; Progress in Polymer Science 35 (2010) 1350-1375. | [2] Jinhong Du, Long Zhao, You Zeng, Lili Zhang, Feng Li, Pengfei Liu, Chang Liu; Comparison of electrical properties between multi-walled carbon nanotube and graphenenanosheet/high density polyethylene composites with a segregated network structure; Carbon 49 (2011) 1094-1100. | [3] Tong Wei, GuilianLuo, Zhuangjun Fan, Chao Zheng, Jun Yan, Chengzhao Yao, Weifang Li, Chen Zhang; Preparation of graphenenanosheet/polymer composites using in situ reduction–extractive dispersion; Carbon 47 (2009) 2290-2299. | [4] GokiEda and Manish Chhowalla; Graphene-based Composite Thin Films for Electronics; Nano Letters (2009) 9(2), 814-818. | [5] Guohua Chen, WenguiWeng, Dajun Wu, Cuiling Wu; PMMA/graphite nanosheets composite and its conducting properties; European Polymer Journal 39 (2003) 2329-2335. | [6] KeXu, DaniloErricolo, MitraDutta, Michael A. Stroscio; Electrical conductivity and dielectric properties of PMMA/graphite nanoplatelet ensembles; Superlattices and Microstructures, 51 (2012) 606-612. | [7] T. Ramanathan, S. Stankovich, D.A. Dikin, H. Liu, H. Shen, S.T. Nguyen, and L.C. Brinson; Graphitic Nanofillers in PMMA Nanocomposites - An Investigation of Particle Size and Dispersion and Their Influence on Nanocomposite Properties; Journal of Polymer Science: Part B: Polymer Physics, 45 (2007), 2097-2112. | [8] Huan Pang, Tao Chen, Gangming Zhang, BaoqingZeng, Zhong-Ming Li; An electrically conducting polymer/graphene composite with a very low percolation threshold; Materials Letters 64 (2010) 2226-2229. | [9] Sourov Chandra, Sourav Bag, Pradip Das, Dipsikha Bhattacharya, Panchanan Pramanik; Fabrication of magnetically separable palladium–graphenenanocomposite with unique catalytic property of hydrogenation; Chemical Physics Letters 519-520 (2012) 59-63. | [10] Dhananjay S. Bodas, S.K. Mahapatra, S.A. Gangal; Comparative study of spin coated and sputtered PMMA as an etch mask material for silicon micromachining; Sensors and Actuators A 120 (2005) 582-588. | [11] Polymer Nanocomposites, Ed. Yiu-Wing Mai and Zhong-Zhen Yu, Woodhead Publishing and Maney Publishing, CRC Press Boca Raton Boston New York Washington, DC (2006) | [12] S. M. Dakka,TG/DTA/MS of poly(methyl methacrylate)-The effect of particle size, Journal of Thermal Analysis and Calorimetry, 74 (2003) 729–734 | [13] Manasi Singhi, M. Fahim; Dielectric Properties of Nanographite-Filled PMMA Composites Prepared by In Situ Polymerization; Polymer Composites 33(5) (2012) 675-682. | [14] R J Sengwa and Shobhna Choudhary, Dielectric properties and structural dynamics of melt compounded hot-pressed poly(ethylene oxide)–organophilic montmorillonite clay nanocomposite films, Bull. Mater. Sci., 35(1)(2012), pp. 19–25 | [15] Ilona Plesa, Florin Ciuprina, and Petru V. Notingher, Dielectric Spectroscopy of Epoxy Resin with and without Inorganic Nanofillers, Journal of Advanced Research in Physics 1(1), (2010) 011011 | [16] G.D. Liang, S.C. Tjong, Electrical properties of low-density polyethylene/multiwalled carbon nanotube nanocomposites, Materials Chemistry and Physics 100 (2006) 132–137 | [17] Fangming Du, Robert C. Scogna, Wei Zhou, Stijn Brand, John E. Fischer, and Karen I. Winey, Nanotube Networks in Polymer Nanocomposites: Rheology and Electrical Conductivity, Macromolecules 37 (2004), 9048-9055 |